

Pyrolysis Mechanisms of Quinoline and Isoquinoline with Density Functional Theory*

LING Lixia (凌丽霞), ZHANG Riguang (章日光), WANG Baojun (王宝俊)** and XIE Kechang (谢克昌)

Key Laboratory of Coal Science and Technology (Taiyuan University of Technology), Ministry of Education and Shanxi Province, Taiyuan 030024, China

Abstract The pyrolysis mechanisms of quinoline and isoquinoline were investigated using the density functional theory of quantum chemistry, including eight reaction paths and a common tautomeric intermediate 1-indene imine. It is concluded that the conformational tautomerism of the intermediate decides the pyrolysis products (C_6H_6 , $HC\equiv C-C\equiv N$, $C_6H_5C\equiv N$ and $HC\equiv CH$) to be the same, and also decides the total disappearance rates of the reactants to be the same, for both original reactants quinoline and isoquinoline during the pyrolysis reaction. The results indicate that the intramolecular hydrogen migration is an important reaction step, which often appears in the paths of the pyrolysis mechanism. The activation energies of the rate determining steps are obtained. The calculated results are in good agreement with the experimental results.

Keywords quinoline, isoquinoline, coal, pyrolysis mechanism, density functional theory

1 INTRODUCTION

Emission of nitrogen oxides (NO , NO_2 and N_2O) in the utilization process of coal is an important environmental problem [1]. It is well known that the presence of nitrogen in coal and coal-derived products is mainly in the form of heterocycles such as pyrrole and pyridine ring systems [2, 3]. Pyrrole, pyridine, indole and quinoline are commonly selected as N-containing model compounds in coal. Many detailed experimental and theoretical studies on the pyrolysis of pyrrole [4–9], pyridine [10–13] and indole [14, 15] have been carried out. Quinoline and isoquinoline, both the molecules containing a pyridine ring fused to benzene, are more authentic than pyridine for describing the coal pyrolysis, considering the actual structures of N-containing components in the aromatic matrix of coal.

To date, there have been some experimental studies on the pyrolysis of quinoline and isoquinoline. In the earlier research, the pyrolysis of quinoline and isoquinoline was studied at 923–1223 K by Patterson *et al.* [16] to evaluate the relative stabilities. Bruinsma *et al.* [17] investigated the pyrolysis of quinoline in a flow reactor, and it was concluded that quinoline was more stable and benzene was identified as one of pyrolysis products. Furthermore, benzonitrile was observed as a pyrolysis product of quinoline [18]. However, the kinetic data for distribution of pyrolysis products or for the pyrolysis mechanism were absent in their experiments. Laskin and Lifshitz [19] investigated the pyrolysis of quinoline and isoquinoline in single pulse shock tube over the temperature range of 1275–1700 K in detail. The experimental results showed that pyrolysis products were $HC\equiv CCN$, C_6H_6 , C_2H_2 and C_6H_5CN , and the total disappearance rates

of quinoline and isoquinoline were the same, whether the reactant was quinoline or isoquinoline. The tautomerism between quinoline and isoquinoline did not occurred, neither traces of isoquinoline in shock heated mixture of quinoline nor traces of quinoline in shock heated mixture of isoquinoline were found. To illustrate this fact, 1-indene imine radical was assumed as an important intermediate, and the pyrolysis mechanisms of quinoline and isoquinoline *via* the intermediate were proposed. Meanwhile, Winkler *et al.* [20] investigated the continuous flow pyrolysis of quinoline and isoquinoline at 1173 K, the same major products as those of Laskin and Lifshitz [19] were identified by gas chromatography-mass spectrometry (GC-MS), and they also agreed with the mechanism proposed by Laskin and Lifshitz.

The presence of 1-indene imine has not been identified experimentally although it is widely believed to be an important intermediate during pyrolysis of quinoline and isoquinoline. In order to better understand the fact that the total disappearance rates of quinoline and isoquinoline are the same and the pyrolysis products are also the same for both reactants, and in order to verify the importance of 1-indene imine intermediate, we carry out a study on the kinetic mechanism of pyrolysis of quinoline and isoquinoline using quantum chemistry calculation.

2 COMPUTATION

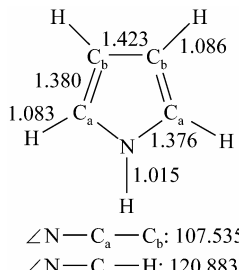
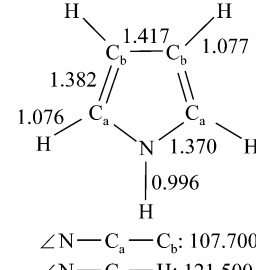
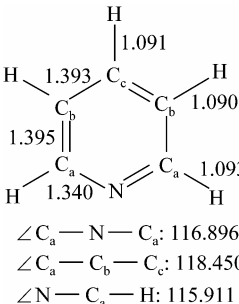
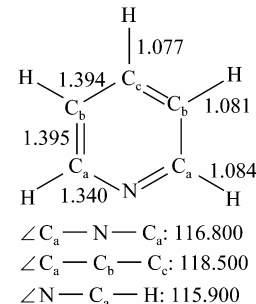
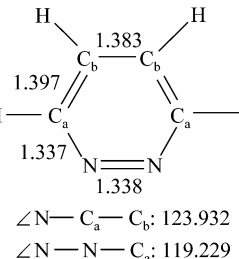
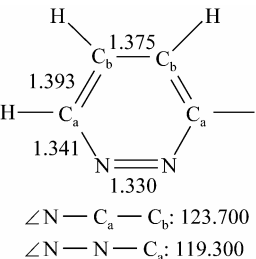
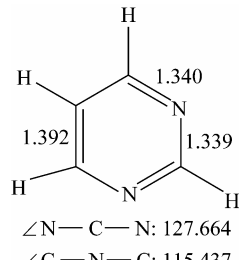
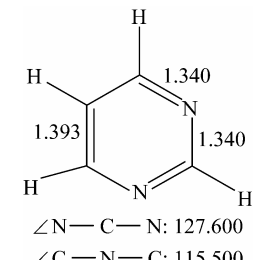
Density functional theory (DFT) method of quantum chemistry calculation was adopted and the calculations were performed using the Dmol³ program [21] mounted on Materials Studio Modeling 4.0 package.

Received 2008-10-23, accepted 2009-07-07.

* Supported by the National Basic Research Program of China (2005CB221203), the National Natural Science Foundation of China (20576087, 20776093) and the Foundation of Shanxi Province (2006011022, 2009021015).

** To whom correspondence should be addressed. E-mail: wangbaojun@tyut.edu.cn

Table 1 The calculated and experimental bond lengths and bond angles of N-containing compounds

N-containing compound	Calculated results	Experimental results	Experimental method
pyrrole	 <p> $\angle N-C_1-C_2: 107.535$ $\angle N-C_1-H: 120.883$ </p>	 <p> $\angle N-C_1-C_2: 107.700$ $\angle N-C_1-H: 121.500$ </p>	MW
pyridine	 <p> $\angle C_1-N-C_5: 116.896$ $\angle C_1-C_2-C_3: 118.450$ $\angle N-C_1-H: 115.911$ </p>	 <p> $\angle C_1-N-C_5: 116.800$ $\angle C_1-C_2-C_3: 118.500$ $\angle N-C_1-H: 115.900$ </p>	MW
pyridazine	 <p> $\angle N-C_1-C_2: 123.932$ $\angle N-N-C_1: 119.229$ </p>	 <p> $\angle N-C_1-C_2: 123.700$ $\angle N-N-C_1: 119.300$ </p>	MW+ED
pyrimidine	 <p> $\angle N-C-N: 127.664$ $\angle C-N-C: 115.437$ </p>	 <p> $\angle N-C-N: 127.600$ $\angle C-N-C: 115.500$ </p>	ED

Note: MW is the abbreviation of microwave spectroscopy; ED is the abbreviation of electron diffraction. Bond lengths are in angstroms ($1\text{ \AA} = 0.1\text{ nm}$) and angles in degrees.

Generalized gradient approximation (GGA) with PW91 function [22] was adopted. The DND basis set, equivalent in accuracy to the 6-31G* Gaussian orbital basis set, was also used. Spin unrestricted was chosen. Total self-consistent field (SCF) tolerance criteria, integration accuracy criteria and orbital cutoff quality criteria were set at medium. Multipolar expansion was set at octupole.

All the reactants, products and possible intermediates in reaction paths were optimized, and their single point energies (SPE) were determined at the same time. All transition state searches were carried out using the Linear Synchronous Transit/Quadratic Syn-

chronous Transit (LST/QST) method. The vibration analyses about the molecular structure of the species involved in the pyrolysis mechanism were carried out at the same theoretical level to verify whether a stationary point corresponding to the structure was a local minimum (equilibrium structure) or a first-order saddle point (transition state) according to the vibration modes, meanwhile, the corresponding zero-point energies (ZPE) were determined. Transition state confirmation calculation was carried out using the nudged elastic band (NEB) method to confirm that the transition states lead to the desired reactants and products. All calculations were performed in HP Proliant DL

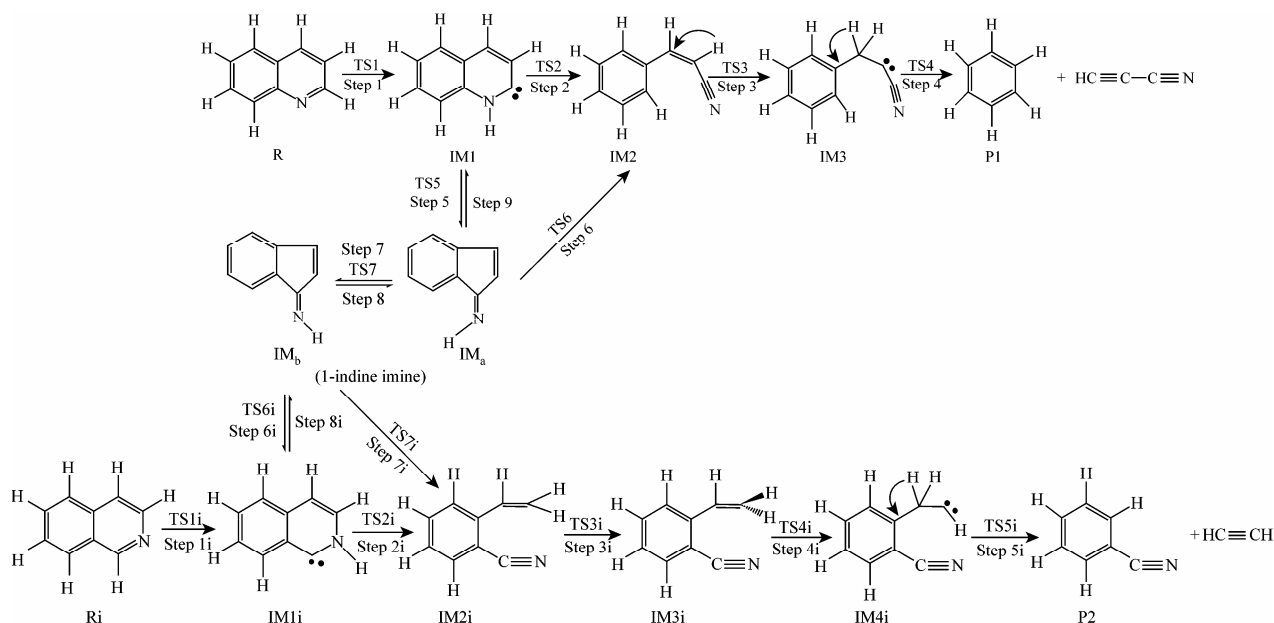


Figure 1 The pyrolysis mechanisms of quinoline (R) and isoquinoline (Ri)

380 G5 server system.

In order to evaluate the reliability of the selected calculation method and parameters, some structural parameters of several N-containing heterocyclic compounds were calculated, and the calculated and experimental results [23] are shown in Table 1. The calculated results are in agreement with the experimental structural parameters, the largest deviation of bond angles is 0.617° , and the deviation of bond lengths is smaller than 0.002 nm. In addition, some results about the reaction mechanism have been obtained using the above method and parameters in our previous studies [24, 25].

3 RESULTS AND DISCUSSION

3.1 The pyrolysis mechanisms of quinoline and isoquinoline

The pyrolysis mechanisms of quinoline and isoquinoline leading to P1 ($\text{HC}\equiv\text{CCN}$, C_6H_6) and P2 (C_2H_2 , $\text{C}_6\text{H}_5\text{CN}$) via 1-indene imine intermediate are proposed in Fig. 1 according to the theoretical calculation. Imaginary frequencies of the transition states in the pyrolysis mechanisms and the bonds corresponding to relative normal vibrations are shown in Table 2. ZPE corrections have been taken into account in this section, and all the numbers cited in the energetic sketch are SPE including the corrections of ZPE.

3.1.1 The paths of quinoline pyrolysis yielding C_6H_6 and $\text{HC}\equiv\text{CCN}$

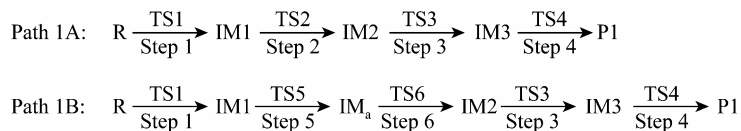
Two possible reaction paths (Path 1A and Path 1B) are found for the pyrolysis: quinoline (R) \rightarrow C_6H_6 + $\text{HC}\equiv\text{CCN}$ (P1), as shown in Scheme 1. The optimized structures and their atomic numbers of reactant, intermediates, transition states and products involved

Table 2 Imaginary frequencies of the transition states and the bonds corresponding to relative normal vibrations

Transition state	Imaginary frequency/ cm^{-1}	Bonds corresponding to normal vibration
TS1	-1875.72	C9—N10—H17
TS2	-1385.26	C4—N10—H17
TS3	-731.35	C8—C7—H16
TS4	-1305.53	C7—C5—H16
TS5	-557.03	C4—C9
TS6	-2077.74	N10—C4—H17
TS7	-1120.31	C9—N10—H17
TS1i	-1887.81	C9—N10—H17
TS2i	-1342.24	C8—N10—H17
TS3i	-1108.85	C8—H16—H17
TS4i	-1948.20	C8—C7—H17
TS5i	-1056.13	C7—C5—H15
TS6i	-602.01	C8—C9
TS7i	-2191.21	C8—N10—H17

in the two paths are shown in Fig. 2, and the relevant energies of the stationary points for Path 1A and Path 1B is shown in Fig. 3.

About Path 1A, we first investigate the direct cleavage mechanism via the formation of *o*-quinoline radical proposed in the two experimental studies [19, 20], the corresponding transition state TS_0 is shown in Fig. 2. The calculation based on the above method and parameters indicates that the activation energy of direct cleavage of bond C9—H17 is $401.09 \text{ kJ}\cdot\text{mol}^{-1}$,



Scheme 1 The reaction schemes for pyrolysis of quinoline (R) leading to P1 (C₆H₆, HC≡CCN)

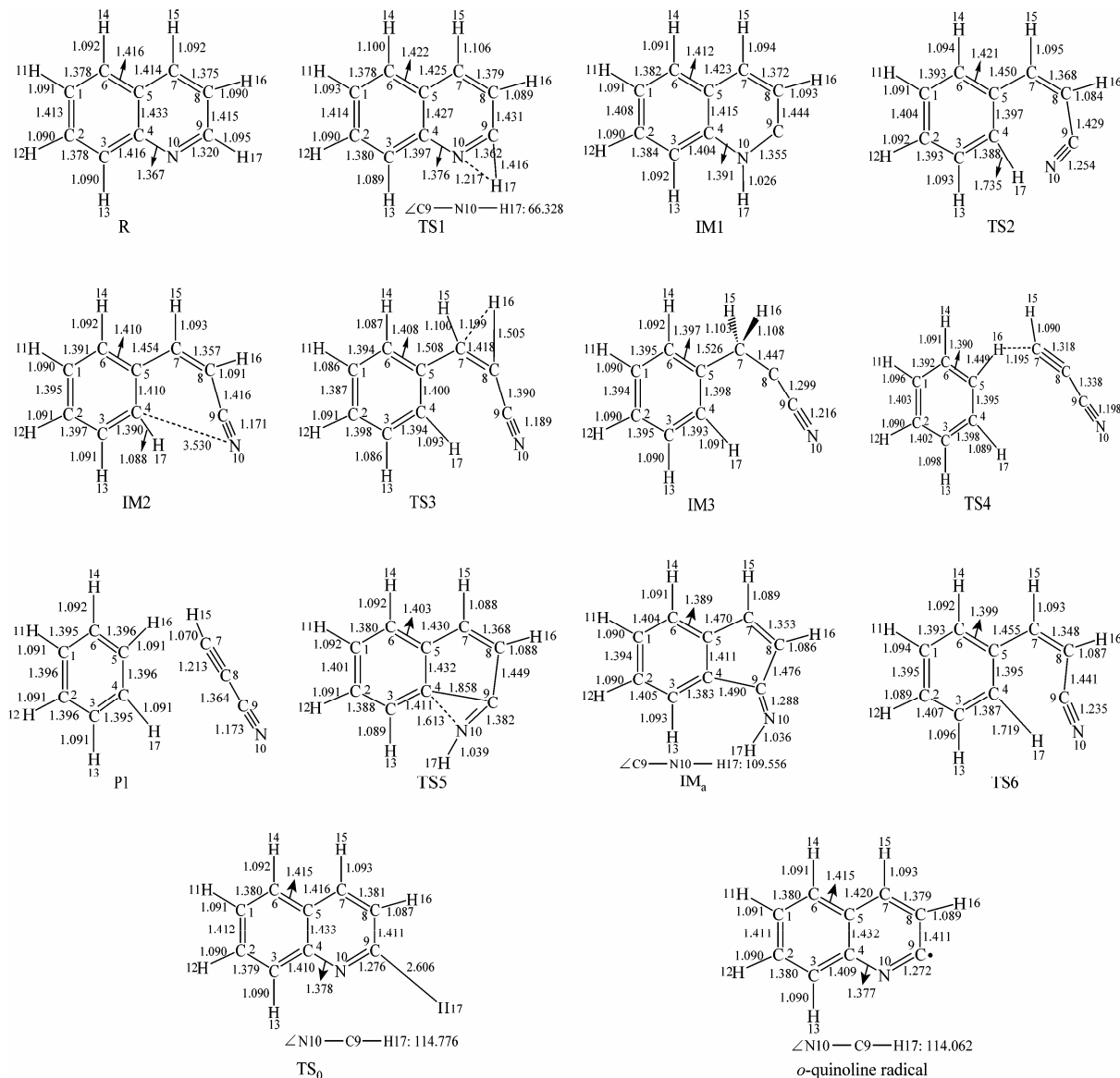


Figure 2 The optimized structures of all species relating to Path 1A and Path 1B [The bond lengths in the figure are in angstroms (1 Å = 0.1 nm) and angles in degrees]

which is about 75 kJ·mol⁻¹ and 85 kJ·mol⁻¹ higher than the experimental activation energy in literatures [17] and [19], respectively. In this study, we suggest that the α -H, H17 in quinoline (R) migrates to N10 to yield IM1. The calculated activation energy of the step *via* TS1 is 344.99 kJ·mol⁻¹, which is close to the experimental activation energy of 326.00 kJ·mol⁻¹ [17] and 316.47 kJ·mol⁻¹ [19]. Thus the theoretical calculation seems to support the proposed hydrogen migration but

not the scheme of direct bond cleavage for the initial step of quinoline pyrolysis. Then H17 in IM1 migrates from N10 to C4 to yield IM2 *via* TS2, followed by a concerted C4-N10 bond cleavage and a change of bond length from 0.1391 nm to 0.3530 nm. This step needs to overcome the energy barrier of 260.50 kJ·mol⁻¹. Finally H16 in IM2 migrates from C8 to C7, sequentially to C5 to yield P1 (C₆H₆, HC≡CCN).

Path 1B has the same initial step to IM1 as Path

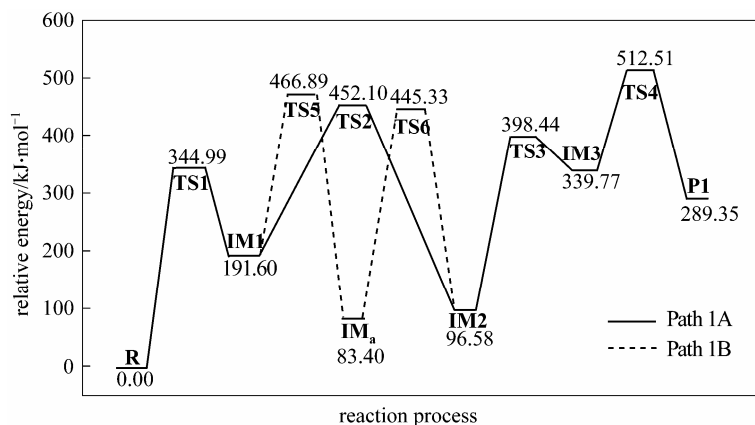
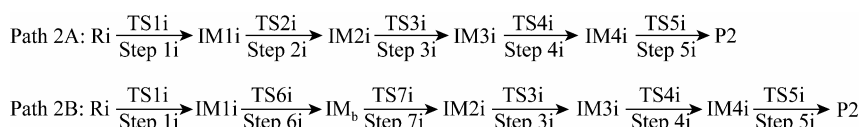


Figure 3 Energetic sketch of the stationary points for Path 1A and Path 1B along the reaction process

[The energy of quinoline (R) is set as the origin of relative energy, whose calculated absolute energy is -401.7474 Ha ($1\text{Ha} = 2625.5$ $\text{kJ}\cdot\text{mol}^{-1}$)]



Scheme 2 The reaction schemes for pyrolysis of isoquinoline (Ri) leading to P2 ($\text{C}_6\text{H}_5\text{CN}$, $\text{HC}\equiv\text{CH}$)

1A. The next step is that the C4 in IM1 links to C9 to yield an intermediate 1-indene imine (IM_a) via TS5, then the migration of H17 in IM_a from N10 to C4 also results in the formation of IM2 with an activation energy of 361.93 $\text{kJ}\cdot\text{mol}^{-1}$. From IM2 to P1, Path 1B and Path 1A have the same steps.

Figure 3 shows that the rate determining steps of Path 1A and Path 1B are Step 1 and Step 6, with activation energies of 344.99 $\text{kJ}\cdot\text{mol}^{-1}$ and 361.93 $\text{kJ}\cdot\text{mol}^{-1}$, respectively. There is only a difference of 16.93 $\text{kJ}\cdot\text{mol}^{-1}$ in the activation energy, so Path 1A and Path 1B may be considered to be the coexistent competitive reaction paths.

3.1.2 The paths of isoquinoline pyrolysis yielding $\text{C}_6\text{H}_5\text{CN}$ and $\text{HC}\equiv\text{CH}$

Two possible reaction paths (Path 2A and Path 2B) are also found for the pyrolysis: isoquinoline (Ri) \rightarrow $\text{C}_6\text{H}_5\text{CN}$ + $\text{HC}\equiv\text{CH}$ (P2), as shown in Scheme 2. The optimized structures and their atomic numbers of all species involved in the two paths are shown in Fig. 4, and the relevant energies of the stationary points for Path 2A and Path 2B are shown in Fig. 5.

Isoquinoline has two α -H (H16 and H17), but their chemical surroundings are different. H16 is always linked to C8 throughout Path 2A, whereas H17 first migrates from C9 to N10 to result in the formation of IM1i. In this step, hydrogen migration destroys the conjugate structure of the N-containing six-membered-ring, so it needs to overcome the higher energy barrier of 338.94 $\text{kJ}\cdot\text{mol}^{-1}$, which is 22.94 $\text{kJ}\cdot\text{mol}^{-1}$ higher than the experimental activation energy [19]. Then H17 in IM1i migrates from N10 to C8 to yield IM2i via TS2i with an activation energy of 265.29 $\text{kJ}\cdot\text{mol}^{-1}$, fol-

lowed by a concerted C8—N10 bond cleavage and a change of bond length from 0.1387 nm to 0.3466 nm.

It is initially proposed that H17 in IM2i migrates from C8 to C7 to yield an intermediate IM4i. However, the transition state conformation calculation indicates that the transition state TS4i can lead directly to IM4i along the reaction process, but not lead to IM2i in the reverse direction, which shows that another intermediate should exist between IM2i and IM4i. By our calculation and analysis, IM3i with a nonplanar geometrical structure is found to be a conformational isomer of IM2i with a planar geometrical structure, which is yield from IM2i via a transition state TS3i. Then IM3i leads to IM4i through the migration of H17. Finally the migration of H15 in IM4i from C7 to C5 results in the formation of P2 ($\text{C}_6\text{H}_5\text{CN}$, $\text{HC}\equiv\text{CH}$).

Path 2B has the same initial step as Path 2A. Then C8 in IM1i links to C9 to yield a more stable intermediate 1-indene imine (IM_b) via TS6i over an energy barrier of 266.20 $\text{kJ}\cdot\text{mol}^{-1}$, and the frequency of C8—C9 stretching vibration of TS6i is calculated to be -602.01 cm^{-1} . IM_b and IM_a are *cis*- and *trans*-conformational tautomers interconverting rapidly via TS7 with an imaginary frequency of -1120.31 cm^{-1} , and corresponding normal vibration is distributed over C9—N10—H17. Then H17 in IM_b migrates from N10 to C8 with an activation energy of 370.76 $\text{kJ}\cdot\text{mol}^{-1}$ via TS7i also to yield IM2i. From IM2i to P2, Path 2B has the same steps as Path 2A.

Figure 5 shows that the rate determining steps of Path 2A and Path 2B are Step 1i and Step 7i, with activation energies of 338.94 $\text{kJ}\cdot\text{mol}^{-1}$ and 370.76 $\text{kJ}\cdot\text{mol}^{-1}$, respectively. There is only a difference of 31.82 $\text{kJ}\cdot\text{mol}^{-1}$ in activation energy, so Path 2A and Path 2B

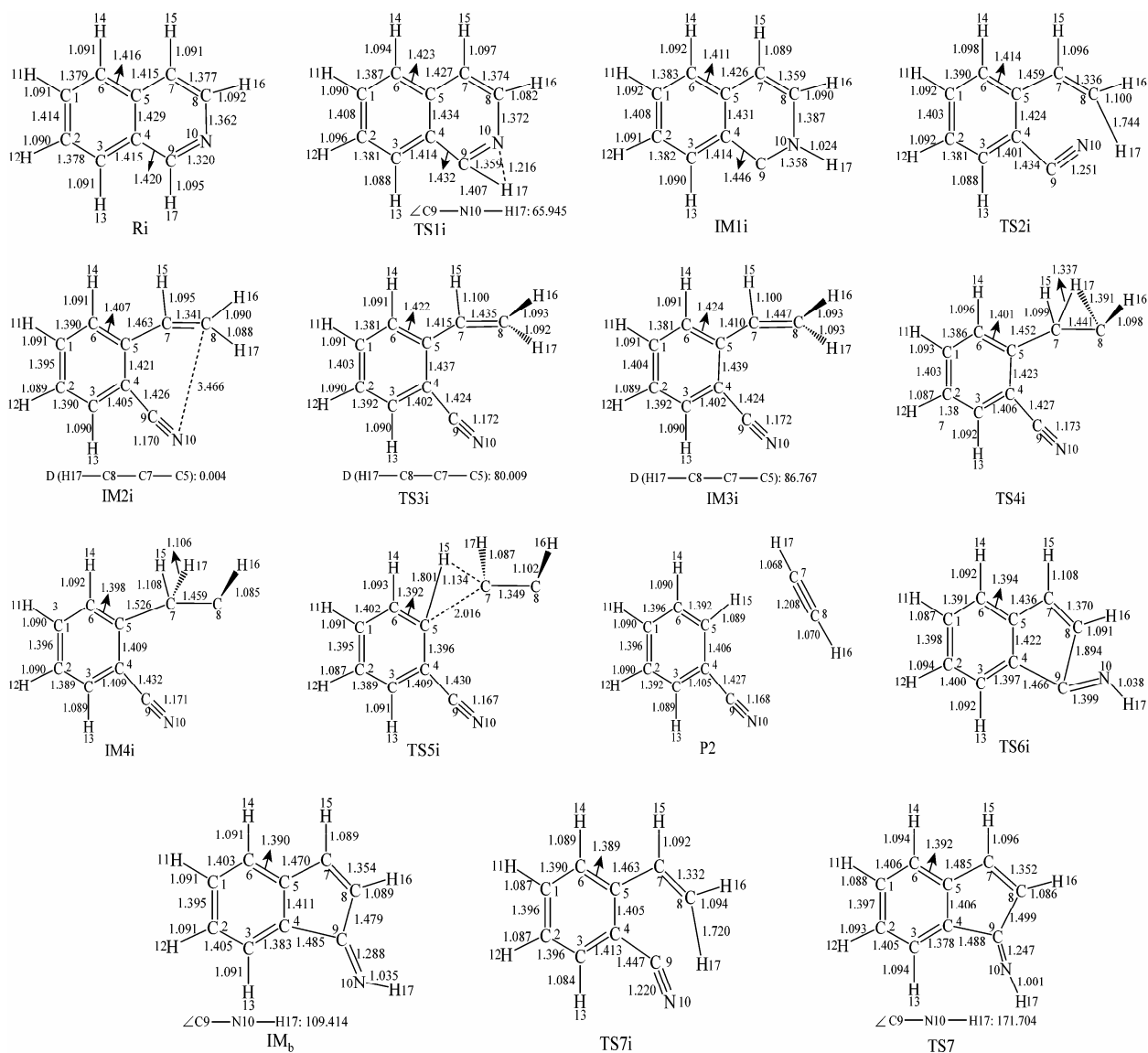


Figure 4 The optimized structures of all species relating to Path 2A and Path 2B [The bond lengths in the figure are in angstroms ($1\text{\AA} = 0.1\text{ nm}$) and angles in degrees]

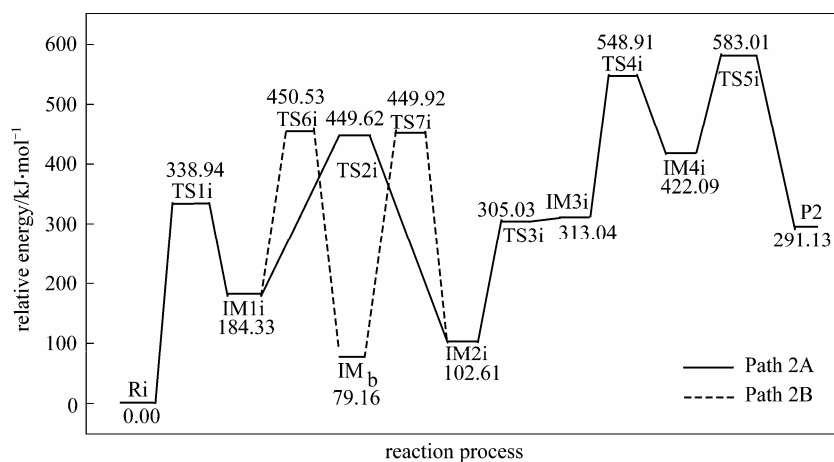


Figure 5 Energetic sketch of the stationary points for Path 2A and Path 2B along the reaction process [The energy of isoquinoline (Ri) is set as the origin of relative energy, whose calculated absolute energy is -401.7458 Ha ($1\text{ Ha} = 2625.5\text{ kJ}\cdot\text{mol}^{-1}$)]

may be considered to be the coexistent competitive reaction paths like the case of Path 1A and Path 1B.

3.1.3 The paths of quinoline pyrolysis yielding C_6H_5CN and $HC\equiv CH$

The formation process of P2 (C_6H_5CN , $HC\equiv CH$) during quinoline pyrolysis has two different paths (Path 3A and Path 3B), which is shown in Scheme 3. All the structures involved in the paths can be seen in Figs. 2 and 4, and the relevant energies of the stationary points for Path 3A and Path 3B are shown in Fig. 6.

Path 3A has the same steps as Path 1B from quinoline (R) to IM_a . Then IM_a goes through a quick conformational tautomerization to IM_b with an activation energy of $113.98 \text{ kJ}\cdot\text{mol}^{-1}$. In Step 7i, H17 in IM_b migrates from N10 to C8 followed by a concerted C8—C9 bond cleavage to yield $IM2i$ with an activation energy of $370.76 \text{ kJ}\cdot\text{mol}^{-1}$. From $IM2i$ to P2, Path 3A has the same steps as Path 2A.

Path 3B has the same steps as Path 3A from quinoline (R) to IM_b . Subsequently, in Step 8i, C8 in IM_b links to N10 followed by a concerted C8—C9 bond cleavage to form $IM1i$ via $TS6i$, which is the reverse reaction of Step 6i, and needs an activation energy of $371.37 \text{ kJ}\cdot\text{mol}^{-1}$. From $IM1i$ to P2, Path 3B and Path 2A have the same steps.

It can be seen from Fig. 6 that the activation en-

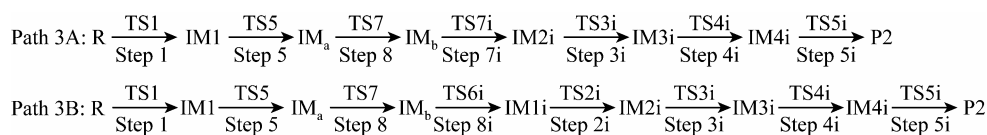
ergies of the rate determining steps are $370.76 \text{ kJ}\cdot\text{mol}^{-1}$ in Path 3A and $371.37 \text{ kJ}\cdot\text{mol}^{-1}$ in Path 3B, so Path 3A and 3B are considered to be the coexistent competitive paths.

3.1.4 The paths of isoquinoline pyrolysis yielding C_6H_6 and $HC\equiv CCN$

The formation process of P1 (C_6H_6 , $HC\equiv CCN$) during isoquinoline pyrolysis also has two different paths (Path 4A and Path 4B), which is shown in Scheme 4. All the structures involved in the paths are listed in Figs. 2 and 4, and the relevant energies of the stationary points for Path 4A and Path 4B are shown in Fig. 7.

Path 4A has the same steps as Path 2B from isoquinoline (Ri) to IM_b , then goes through a quick conformational tautomerization to IM_a with an activation energy of $113.96 \text{ kJ}\cdot\text{mol}^{-1}$. In Step 6, H17 in IM_a migrates from N10 to C4 following by a concerted C4—C9 bond cleavage to form $IM2$ with an activation energy of $361.93 \text{ kJ}\cdot\text{mol}^{-1}$. From $IM2$ to P1, Path 4A and Path 1A have the same steps.

Path 4B has the same steps as Path 4A from isoquinoline (Ri) to IM_a . Subsequently, in Step 9, C4 in IM_a links to N10 followed by a concerted C4—C9 bond cleavage to form $IM1$, which is the reverse reaction of Step 5 and has an activation energy of 383.48



Scheme 3 The reaction schemes for pyrolysis of quinoline (R) leading to P2 (C_6H_5CN , $HC\equiv CH$)

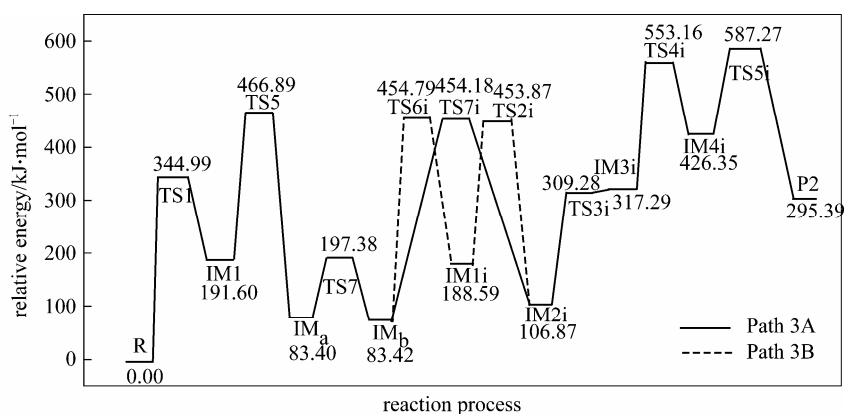
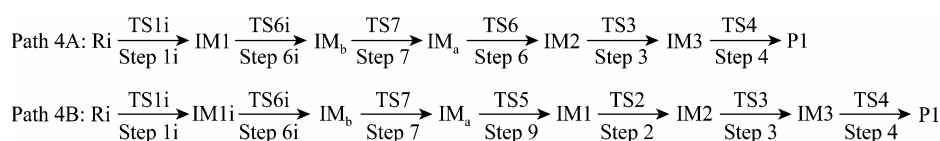


Figure 6 Energetic sketch of the stationary points for Path 3A and Path 3B along the reaction process

[The energy of quinoline (R) is set as the origin of relative energy, whose calculated absolute energy is -401.7474 Ha ($1\text{Ha} = 2625.5 \text{ kJ}\cdot\text{mol}^{-1}$)]



Scheme 4 The reaction schemes for pyrolysis of isoquinoline (Ri) leading to P1 (C_6H_6 , $HC\equiv CCN$)

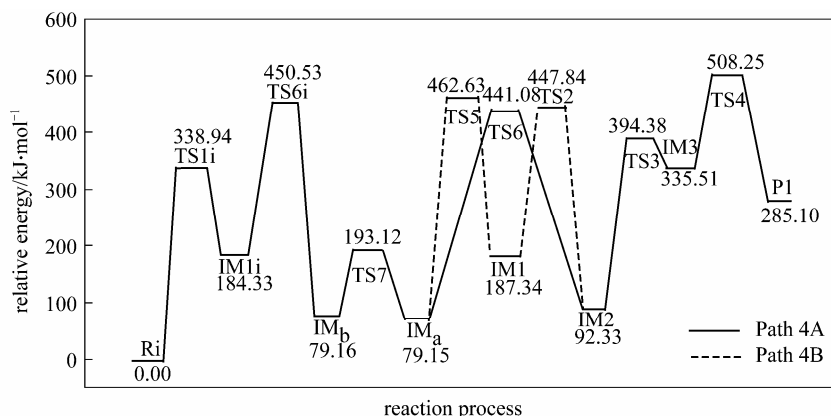


Figure 7 Energetic sketch of the stationary points for Path 4A and Path 4B along the reaction process

[The energy of isoquinoline (Ri) is set as the origin of relative energy, whose calculated absolute energy is -401.7458 Ha (1 Ha = 2625.5 kJ·mol $^{-1}$)]

kJ·mol $^{-1}$. From IM1 to P1, Path 4B and Path 1A have the same steps.

It can be seen from Fig. 7 that the activation energies of rate determining steps are 361.93 kJ·mol $^{-1}$ in Path 4A and 383.48 kJ·mol $^{-1}$ in Path 4B, so Path 4A and 4B may be considered to be the coexistent competitive paths.

3.1.5 The analysis of total reaction paths

According to the above analysis of every path, it can be concluded that the most feasible formation processes of P1 (C_6H_6 , $HC\equiv C-C\equiv N$) and P2 ($C_6H_5C\equiv N$, $HC\equiv CH$) during quinoline and isoquinoline pyrolysis should involve two parts: leading to the intermediate 1-indene imine with two conformational tautomers, and yielding P1 and P2 from the common intermediate.

Quinoline goes through three paths (Path 1B, Path 3A and Path 3B) towards IM_a and isoquinoline goes through other three paths (Path 2B, Path 4A and Path 4B) towards IM_b by the kinetic mechanism involving the intramolecular hydrogen migration, in which the highest energy barriers of 344.99 kJ·mol $^{-1}$ in Step 1 and 338.94 kJ·mol $^{-1}$ in Step 1i have to be overcome, which are close to the experimental activation energies 326.00 kJ·mol $^{-1}$ [17] and 316.47 kJ·mol $^{-1}$ [19]. Because of the similar activation energies, the production rates of 1-indene imine are almost the same, whether the original reactant is quinoline or isoquinoline. Then there is a quick conformational tautomeric equilibrium between IM_a and IM_b with activation energies of 113.98 kJ·mol $^{-1}$ and 113.96 kJ·mol $^{-1}$.

The common intermediate 1-indene imine goes through three paths (Path 1B, Path 4A and Path 4B) towards P1, and other three paths (Path 2B, Path 3A and Path 3B) towards P2. The calculated results show that the highest energy barriers yielding P1 and P2 are 361.93 kJ·mol $^{-1}$ in Step 6 and 370.76 kJ·mol $^{-1}$ in Step 7i. The highest energy barriers are almost the same, slightly higher than the experimental results [17, 19]. Thus it is concluded that the total disappearance rates

of quinoline and isoquinoline are the same, and the composition of the pyrolysis products is also the same, no matter the original reactant is quinoline or isoquinoline, which is in agreement with the experimental results [19, 20].

3.2 The role of 1-indene imine during quinoline and isoquinoline pyrolysis

A common intermediate 1-indene imine is yielded from IM1 and IM1i in the pyrolysis mechanisms of quinoline and isoquinoline, which has two conformational tautomers (IM_a and IM_b) according to our theoretical calculation. There are two tautomeric structures of 1-indene imine so that H17 linked to N10 could migrate to C4 or C8, one of the two neighboring carbon atoms, *via* TS6 or TS7i to IM2 or IM2i, respectively. Then, the reaction leads to the formation of P1 (C_6H_6 , $HC\equiv C-C\equiv N$) and P2 ($C_6H_5C\equiv N$ and $HC\equiv CH$) through the subsequent several paths. This analysis may explain why the composition of the pyrolysis products is the same whether the original reactant is quinoline or isoquinoline during the pyrolysis. It shows that 1-indene imine intermediate plays a central role in the formation of the products during quinoline and isoquinoline pyrolysis.

4 CONCLUSIONS

The kinetic mechanisms of pyrolysis of quinoline and isoquinoline are investigated in detail using the density functional theory of quantum chemistry. The results are summarized as follows:

(1) A rational reaction mechanism involving eight reaction paths and a common tautomeric intermediate is proposed, and the activation energies of the rate determining steps are obtained. The calculated results are in good agreement with the experimental results.

(2) The conformational tautomerism of 1-indene imine intermediate plays an important role in the

mechanism, which decides the composition of the pyrolysis products to be the same, and also decides the total disappearance rates of the reactants to be the same, whether the original reactant is quinoline or isoquinoline.

(3) The intramolecular hydrogen migration is an important reaction step, which appears widely in the paths of the pyrolysis mechanism.

REFERENCES

- 1 Tan, L.L., Li, C.Z., "Formation of NO_x and SO_x precursors during the pyrolysis of coal and biomass. Part I. Effects of reactor configuration on the determined yields of HCN and NH₃ during pyrolysis", *Fuel*, **79**, 1883–1889 (2000).
- 2 Kelemen, S.R., Gorbaty, M.L., Kwiatek, P.J., Fletcher, T.H., Watt, M., Solum, M.S., Pugmire, R.J., "Nitrogen transformations in coal during pyrolysis", *Energ. Fuel*, **12**, 159–173 (1998).
- 3 Solomon, P.R., Colket, M.B., "Evolution of fuel nitrogen in coal devolatilization", *Fuel*, **57**, 749–755 (1978).
- 4 Mackie, J.C., Colket, M.B., Nelson, P.F., Esler, M., "Shock tube pyrolysis of pyrrole and kinetic modeling", *Int. J. Chem. Kinet.*, **23**, 733–760 (1991).
- 5 Lifshitz, A., Tamburu, C., Suslensky, A., "Isomerization and decomposition of pyrrole at elevated temperatures. Studies with a single-pulse shock tube", *J. Phys. Chem.*, **93**, 5802–5808 (1989).
- 6 Dubnikova, F., Lifshitz, A., "Isomerization of pyrrole. Quantum chemical calculations and kinetic modeling", *J. Phys. Chem. A*, **102**, 10880–10888 (1998).
- 7 Zhai, L., Zhou, X.F., Liu, R.F., "A theoretical study of pyrolysis mechanisms of pyrrole", *J. Phys. Chem. A*, **103**, 3917–3922 (1999).
- 8 Martoprawiro, M., Bacsakay, G.B., Mackie, J.C., "Ab initio quantum chemical and kinetic modeling study of the pyrolysis kinetics of pyrrole", *J. Phys. Chem. A*, **103**, 3923–3934 (1999).
- 9 Bacsakay, G.B., Martoprawiro, M., Mackie, J.C., "The thermal decomposition of pyrrole: An ab initio quantum chemical study of the potential energy surface associated with the hydrogen cyanide plus propyne channel", *Chem. Phys. Lett.*, **300**, 321–330 (1999).
- 10 Mackie, J.C., Colket, M.B., Nelson, P.F., "Shock tube pyrolysis of pyridine", *J. Phys. Chem.*, **94**, 4099–4106 (1990).
- 11 Memon, H.U.R., Bartle, K.D., Taylor, J.M., Williams, A., "The shock tube pyrolysis of pyridine", *Int. J. Energ. Res.*, **24**, 1141–1159 (2000).
- 12 Liu, R.F., Huang, T.T.S., Tittle, J., Xia, D.H., "A theoretical investigation of the decomposition mechanism of pyridyl radicals", *J. Phys. Chem. A*, **104**, 8368–8374 (2000).
- 13 Ninomiya, Y., Dong, Z.B., Suzuki, Y., Koketsu, J., "Theoretical study on the thermal decomposition of pyridine", *Fuel*, **79**, 449–457 (2000).
- 14 Laskin, A., Lifshitz, A., "Isomerization and decomposition of indole. Experimental results and kinetic modeling", *J. Phys. Chem. A*, **101**, 7787–7801 (1997).
- 15 Zhou, X.F., Liu, R.F., "A density functional theory study of the pyrolysis mechanisms of indole", *J. Mol. Struct. Theochem.*, **461/462**, 569–579 (1999).
- 16 Patterson, J.M., Issidorides, C.H., Papadopoulos, E.P., Smith, Jr. W.T., "The thermal interconversion of quinoline and isoquinoline", *Tetrahedron. Lett.*, **15**, 1247–1250 (1970).
- 17 Bruinsma, O.S.L., Tromp, P.J.J., De Sauvage Nolting, H.J.J., Moulijn, J.A., "Gas phase pyrolysis of coal-related aromatic compounds in a coiled tube flow reactor 2. Heterocyclic compounds, their benzo and dieno derivatives", *Fuel*, **67**, 334–340 (1988).
- 18 Axworthy, A.E., Dayan, V.H., Martin, G.B., "Reactions of fuel-nitrogen compounds under conditions of inert pyrolysis", *Fuel*, **57**, 29–35 (1978).
- 19 Laskin, A., Lifshitz, A., "Thermal decomposition of quinoline and isoquinoline. The role of 1-indene imine radical", *J. Phys. Chem. A*, **102**, 928–946 (1998).
- 20 Winkler, J.K., Karow, W., Rademacher, P., "Gas phase pyrolysis of heterocyclic compounds (3) Flow pyrolysis and annulation reaction of some nitrogen heterocycles. A product oriented study", *ARKIVOC*, **1** (4), 576–602 (2000).
- 21 Delley, B., "From molecules to solids with the Dmol³ approach", *J. Chem. Phys.*, **113** (18), 7756–7764 (2000).
- 22 Perdew, J.P., Chevary, J.A., Vosko, S.H., Fiolhais, C., "Atoms, molecules, solids and surfaces: Application of the generalized gradient approximation for exchange and correlation", *Phys. Rev. B*, **46** (11), 6671–6687 (1992).
- 23 Lide, D.R., *Handbook of Chemistry and Physics*, 82nd edition, CRC Press, New York, 9–40 (2001–2002).
- 24 Zhao, L.J., Ling, L.X., Zhang, R.G., Liu, X.F., Wang, B.J., "Theoretical study on pyrolysis mechanism of O-containing model compound anisole in coal", *J. Chem. Ind. Eng. (China)*, **59** (8), 2095–2102 (2008). (in Chinese)
- 25 Zhang, R.G., Huang, W., Wang, B.J., "Theoretical calculation for interaction of CO₂ with ·H and ·CH₃ in synthesis of acetic acid from CH₄ and CO₂", *Chin. J. Catal. (China)*, **28** (7), 641–645 (2007). (in Chinese)